UNIVERSITÉ DE GENÈVE
FACULTY OF SCIENCE
Department of Astronomy

Searching for planet-planet eclipses

Marchand Maxime, University of Geneva, 1st year Master

Under the supervision of
Deline Adrien, Leleu Adrien, Bourrier Vincent, University of Geneva, Exoplanetology group

Abstract

This report presents the work done in the context of the 1st year Master laboratories in the department of Astronomy of the University of Geneva. A software has been developed in order to propose a tool capable of estimating the probability to observe an eclipse between two exoplanets at a given time. Databases have been used in order to compute those probabilities between early 2023 and end of 2025, showing interesting and encouraging results for some systems.

Contents

1 Introduction

Multi-planetary systems offer the opportunity to study the evolution of solar systems others than our own. For this purpose, an accurate knowledge of the orbital parameters is crucial in order to find pertinent assumptions about the evolution of these systems, both regarding their formation, and their future [1]. In some cases, multi-planetary systems have only one planet that has been observed through transit photometry. Methods have been developed in order to study the co-evolution with the other planets, through transit timing variations, for instance [2, 3]. In the set of systems with multiple transiting exoplanets, some may offer the right configuration such that two planets transiting at the same time overlap each other during their trajectory in front of the stellar disc. Such events are called planet-planet eclipses (PPEs), and are identifiable on the light curves [4, 5], offering exquisite constraints on the calculation of the orbital parameters of the exoplanets. Even if some observations of PPEs have already been made [4, 5], these events are unfortunately extremely rare, and there is no publication in the literature dedicated to the prediction of these events. In this paper, we present a numerical method based on Monte-Carlo sampling providing an estimation of the probability of detection of a planet-planet eclipse.

2 Theoretical elements

We present in this section some fundamental concepts, important notions and definitions that have been used in this work. We introduce the relevant quantities needed to describe exoplanets and explain the methods used in order to measure them.

2.1 Sky coordinates & orbital parameters

In order to describe the orbital parameters of an exoplanet, one has to define the relevant quantities. The *line of sight* is the straight line between the observer and the star. The *sky plane* is chosen to be perpendicular to the line of sight, and include the stellar center. The *orbital plane* corresponds to the plane in which the planet moves during its orbit around the star. The *inclination* i is the angle between the two planes. If the orbital and the sky planes coincide, the inclination is zero, and the system star-planet is *face-on*. On the other hand, if the two planes are perpendicular, the inclination is a right angle and the system is said to be *edge-on*. One defines the *spin-orbit angle* Ψ (also called *true obliquity*) as the angle between the normal vector to the orbital plane and the axis of rotation of the star. The *projected obliquity* λ corresponds to the angle formed by the projection of Ψ on the sky plane.

A planet orbiting around a star forms a two-body interaction system, which solution can be found using Kepler's laws. One can derive that the orbit of the planet around the star forms an ellipse. One defines a as the *semi-major axis*, corresponding to the longest radius of the ellipse. Inversely, one defines b as the *semi-minor axis*, as illustrated in Fig. 1. The shape of the ellipse can be described using the *eccentricity*, which is a number quantifying by how much the star is far from the middle of the ellipse, in percentages of a. Looking at the different cases for the values of e, a null eccentricity ($e = 0$) means that the star is in the middle of the ellipse. One can deduce from this configuration that the planet evolves on a circle, meaning that $a = b$. On the other hand eccentricities between 0 and 1 non-included describe elliptical orbits. Eccentricities equal or higher than one do exist, and correspond respectively to parabolic and hyperbolic trajectories. Such configurations do not allow the planet to orbit around the star, as it is just passing, and thus cannot be called star-planet systems.

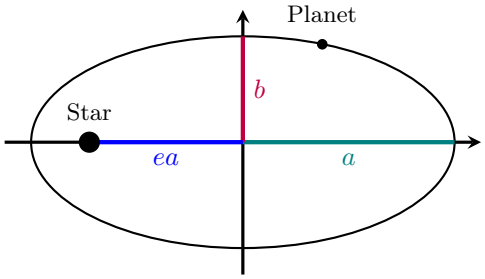

Figure 1: An illustration of the orbit of a planet. The segments a and b are respectively the semi-major and semi-minor axes. The eccentricity of a planet is a positive real number, describing how much the star is far from the center of the ellipse. If $e = 0$, the orbit of the planet is circular. $0 < e < 1$ describes elliptical orbits. If $e = 1$, the planet cannot orbit around the star and describes a parabola. Eccentricities higher than one describe hyperbolic trajectories.

2.2 Transit method

Transit method appears to be the most prolific method to detect exoplanets. It consists of continuously measuring the brightness of a star. When an exoplanet is transiting on the stellar disc (meaning that it is passing between the star and the observer), one detects a decrease of the intensity in the light curve [6]. This effect is due to the fact that a part of the star is hidden by the planetary disc. This phenomenon is illustrated in Fig. 2. In addition to confirming the presence of an exoplanet, the shape of the light curve contains a lot of information, both regarding the dimensions of the planet, and its orbital parameters. As illustrated in Fig. 2, one defines the *mid-transit time* T_0 as the time where the plan-

etary disc is closest to the centre of the projected stellar disc. T_{14} corresponds to the *transit duration*, namely the time between the entry and exit of the planet on the stellar disc. The *transit depth* D quantifies the loss in brightness due to the transit of the planet. This quantity allows us to compute the ratio between the radii of the planet and the star.

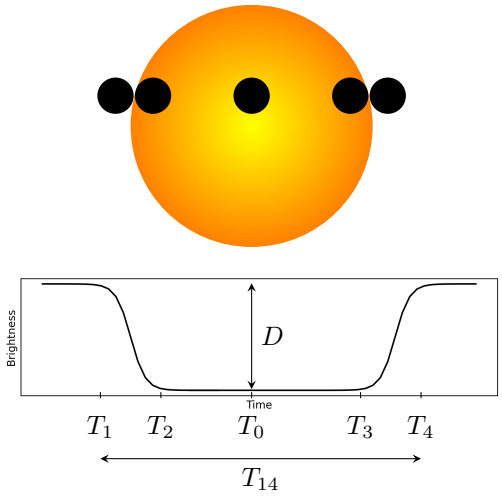

Figure 2: An illustration of the transit method. On the top, a scheme illustrating the transit of a planet. Below is represented a theoretical transit light curve. One clearly identifies the transit of the planet through the decrease of the measured brightness. D is defined as the transit depth, and gives information about the ratio between the two radii of the star and the planet. T_0 is the mid-transit time, where the planetary disc is closest to the centre of the stellar disc. One defines T_1, T_2, T_3, T_4 such that T_1 is the time where the planetary disc begins to transit on the stellar disc, and T_2 when the planet totally entered in the stellar disc. The time interval T_{12} is called the ingress duration. Same definitions for T_3 and T_4, when the planet leaves the stellar disc. The time interval T_{34} is called the egress duration. The time interval between T_1 and T_4 is called the transit duration and is denoted by T_{14}.

Of course, this method aims to be used for edge-on systems[1], otherwise the planet will not pass between the star and the observer, and it will not create a transit light curve. A lot more information, which is not illustrated in Fig. 2 for the sake of clarity, can be deduced from the shape of the light curve. During the transit time, the light curve can be slightly curved due the Limb-darkening (the brightness of the stellar disc is stronger in the middle than near the edge) [7]. Also, just before that the planet passes behind the star, the light curve can slightly increase, because in addition of the received luminosity of the star, one also detects the dayside of the planet, corresponding to the reflected light of the star on the planet [6].

2.3 The Rossiter-McLaughlin effect

The rotation of the star can also be used in order to obtain some information on the orbital parameters. Assuming a star which rotation axis is included in the sky plane, and points to the upper direction, the left part of the star will be moving toward the observer, resulting in a blueshift of the received spectra. The inverse occurs for the right side of the star moving away from the observer, that will be redshifted. The total area that it blueshifted is the same as the redshifted one. Assuming that the planet travels from the left to the right, it will first hide a zone of the star that is blueshifted, resulting in an excess of redshift, and vice versa when the planet will cover a redshifted zone. This phenomenon is called the Rossiter-McLaughlin effet [8] and can be detected by measuring an anomaly in the apparent radial velocity of the star, using spectroscopy, as illustrated in Fig. 3. The shape of this residual radial velocity curve allows us to deduce the obliquity of the planet.

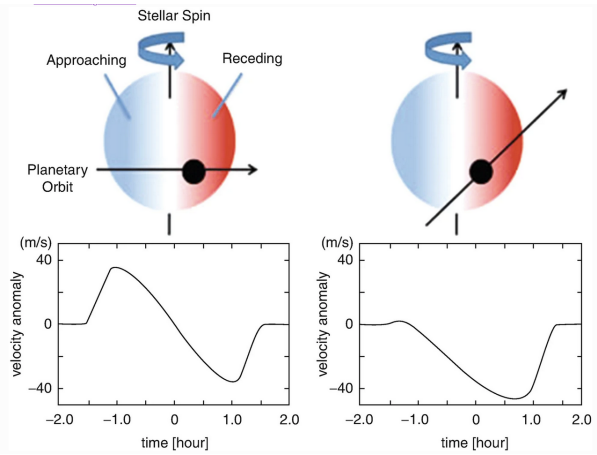

Figure 3: An illustration of the Rossiter-McLaughlin effect, for two different configurations of the planetary orbit. On the top, the star is rotating, resulting in a blueshift of the left side and a redshift of the right side. At the bottom is illustrated the corresponding residual anomaly of the radial velocity curve of the star. Then the planet is transiting, its position on a blueshifted area will create an excess of redshift, and vice versa. The shape of this plot allows to deduce the projected obliquity λ. Figure taken from [8].

2.4 PPEs detection on the light curve

We now have all the tools to make the link between planet-planet eclipses and transit method, and understand why they present some interest in the study of the orbital parameters. A planet-planet eclipse occurs when two exoplanets are transiting at the same time on the stellar disc and cross each other at a certain time, as illustrated in Fig. 4. One of the most important aspect of PPEs is that these events can be detected in the transit light curve.

[1] In this paper, the word system refers to a star and its planet(s).

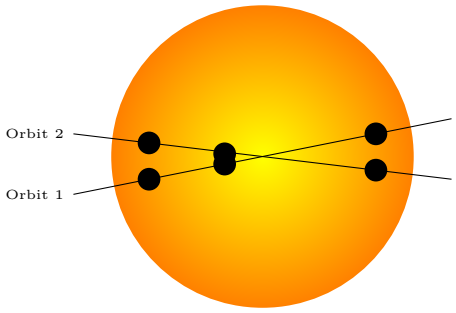

Figure 4: An illustration of a planet-planet eclipse. Two transiting exoplanets are shown, at three different times of their transit. A PPE occurs when these two planets cross each other on the stellar disc.

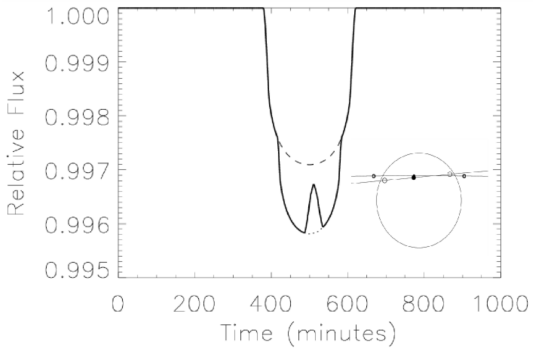

(A)

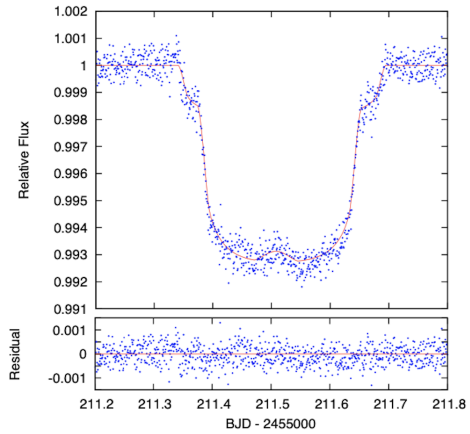

(B)

Figure 5: **(A)** A theoretical light curve with detection of a PPE. The dashed line represents the shape of the light curve if there were only one planet transiting. The dotted line represents the shape of the light curve with two planets, without overlapping. Finally, the solid line illustrates the transit light curve with a PPE occuring. One can identify the bump around $t = 500$ min. This figure is taken from [1]. **(B)** An example of a real transit light curve measurement with detection of a PPE for the star KOI-94 between planets 01 and 03. One can identify all the elements presented in Fig. **(A)**. This figure is taken from [4].

Indeed, let us suppose that two planets have entered on the stellar disc. One might expect that the two ingress and egress durations are visible on the light curve. The size of the transit depth D is now linked to the total area of the two planetary discs. At the moment where the two planets will cross, the two discs will overlap each other, resulting in the fact that the total area covering the star will be smaller than the sum of the two discs. This phenomenon is characterised by a *bump* on the light curve, as illustrated in Fig. 5. The presence of this bump is what makes PPEs very interesting for the research in multi-planetary systems formation and evolution. Indeed, this additional information on the light curve provides exquisite constraints on the orbital parameters of the exoplanets. As the bump allows to assert that the two planetary discs are very close to each other. Knowing the time at which this bump appears allows to obtain much more precise estimations for the values of the orbital parameters. This phenomenon can be used as an anchor point that allows to exclude a part of the possible values for the orbital parameters and thus allows to reduce the uncertainties on these quantities.

3 Method

We now present the method used in order to compute the probabilities of planet planet eclipses.

3.1 Selection of the planets

Before computing the probabilities, the list of exoplanets[2] has been filtered in order to keep the best candidates for the computations. As we are interested in looking for planet-planet eclipses, we only considered the planets where the radius and their upper and lower errors where known. By doing so, we are assured that the planet has been observed once with the transit method. We also paid attention to keep the systems including two exoplanets or more. As discussed in the next section, the computation of the probabilities will be done using trigonometry, we thus only want to keep the planets where the eccentricity is small enough to consider that the planet has a circular orbit. Considering the errors on the eccentricities, we concluded that planets having an eccentricity not higher than 0.2 could be used in the code without losing too much precision. For a set of planets, the value of the transit duration T_{14} was not known. In order to use them, we used the following approximation formula :

$$T_{14} \sim \frac{P}{\pi} \arcsin\left(\frac{\sqrt{\left(1+\frac{R_p}{R_*}\right)^2 - b^2}}{\frac{a}{R_*}}\right) \quad (1)$$

[2] See Section 4 for more details on the data that hes been used.

Where P is the period of the planet, R_p and R_* are respectively the radii of the planet and the star, a is the semi-major axis of the orbit and $b = \frac{a}{R_*}\cos(i)$ is the impact parameter.

3.2 Selecting the time windows

In this project, we are interested to compute the probabilities of planet planet eclipses on all the database, and decided to compute them on a time interval of two or three years, between 2023 and 2026. Regarding the ratio between this duration, and the time intervals where the planets are transiting on the stellar disc, it is clearly not worth it to make the computation on all this duration. We thus decided to select small time intervals, during which we know that one of the two planets is transiting. In order to be sure to include the two transits, we computed these time windows using the orbital parameters of the planet having the longest period.[3] More formally, knowing the period P, the mid-transit time T_0 and the transit duration T_{14}, we are able to compute the set

$$\Sigma \equiv \{n \in \mathbb{N} \mid T_0 + nP \in \Delta T_{obs}\} \tag{2}$$

where ΔT_{obs} is the time interval in which we want to compute the probabilities. In other words, we computed all the mid-transit times of the planet in the time window ΔT_{obs}. For each of these values, we generated a time grid $[-\Delta t, \Delta t]$, of small time increments dt. In our code, we choosed $\Delta t = 0.6 \cdot T_{14}$, in order to cover the transit duration despite the uncertainties on the transit duration, and $dt = 30$ sec as a compromise between the time of a PPE detection (~ 1 min) and the computation time.

3.3 Monte-Carlo sampling

The data set that we want to use in order to compute the probabilities raises two difficulties :

1. The orbital parameters are known up to a certain degree of confidence (errors on the data)
2. These errors are increasing as we want to explore time intervals more and more distant in time (this can be seen directly from Eq. (2), for instance).

In order to work around these problems, and get reasonable results, we created a Monte-Carlo sampling on every orbital parameters of both planet. In other words, for each orbital parameter Q and its upper and lower errors ΔQ_+ and ΔQ_-, we generated a set of N random values following a normal distribution $Q_i \sim \mathcal{N}(Q, \sigma)$, centred on Q, and whose standard deviation is given by $\sigma = \sqrt{\frac{\Delta Q_+^2 + \Delta Q_-^2}{2}}$. In our code, we chose the number of samples to be $N = 10'000$. For each of these configurations, we compute their evolution in space on the time grid defined in the previous section, and project their position on the sky plane. We then determine if the two planets are overlapping each other according to the following criteria :

1. Both planets are in front of the star (see Fig. 6)
2. The projected euclidean distance between the two planets is smaller than the sum of their radius

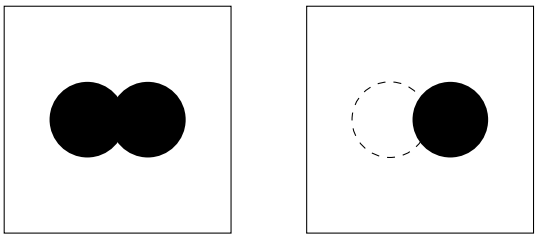

Figure 6: An illustration of the projection of the two planetary discs on the sky plane. The filled circles represent planets in front of the star, and dashed circles represent planets located behind it. As one can see, even if the euclidean distance is smaller in the two cases, one still has to verify that both planets are located in front of the star in order to confirm a PPE that could be observed.

3.4 Computing the probabilities on the whole dataset

The main objective of this project was to compute the probabilities on the whole dataset. Every steps described in the previous section have been applied on each pairs of planets. As the projected spin-orbit angle λ is hard to measure, the vast majority of the pairs did not have the obliquity defined (see Section 4.2). This quantity is crucial for computing the probabilities. We thus only considered the pairs where at least one of the two obliquities was known. In the case where both λ were known, we applied the method as described above. In the other case where one λ was missing, we computed the probabilities five times, assigning five different values of the obliquity :

$$\lambda_2 = \lambda_1 + [\, -90.0^\circ\, , -45.0^\circ\, , 0.0^\circ\, , 45.0^\circ\, , 90.0^\circ\,] \tag{3}$$

[3] By doing so, we are sure that when the planet having the longest period performed one revolution around the star, the other planet will also have made at least one.

4 Data

4.1 Source of the data

The data that has been used for this work has been created by merging two catalogues, namely the Extrasolar Planets Encyclopedia [9] and the Nasa Exoplanets Archive [10]. These catalogs were downloaded on November 30th, 2022. This procedure allowed us to get 2187 planets, for 895 stars.

4.2 Statistics on the data

As mentioned in the Method section, we removed all the planets for which the values of the radius and the upper and lower values were not known, and the ones for which the value of the eccentricity exceeded 0.2. This procedure removed 675 planets. Finally, the remaining systems containing only one planet were not considered, leaving us with a final number of 1408 planets for 560 stars. Fig. 7 illustrates the distribution of the stars according to the number of planets orbiting around them.

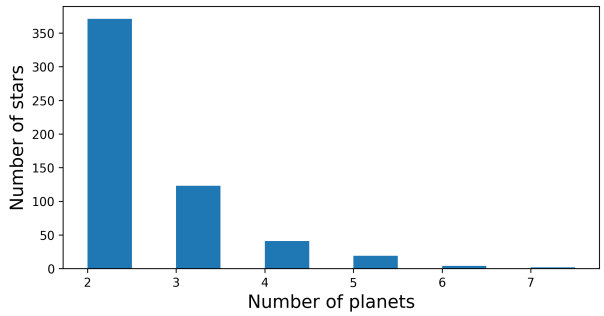

Figure 7: A graphic made with the catalogue used in our code. It illustrates the number of stars, as a function of the number of planets orbiting around them. As one can observe, the vast majority of the stars have one or two planets orbiting. The star having seven planets corresponds to TRAPPIST-1 [11], and will show some interesting results, as it will be mentioned in Sec. 5.

As one can see in Fig. 7, the vast majority of the stars have 2 or three planets orbiting. The star hosting 7 planets is TRAPPIST-1 [11], and will present some interesting results, as it will be discussed in the following section. Fig. 8 illustrates the number of planets as a function of their eccentricity. As one can observe, the values for e are mostly between 0 and 0.2. The graph below represents the eccentricities for the dataset that has been filtered.

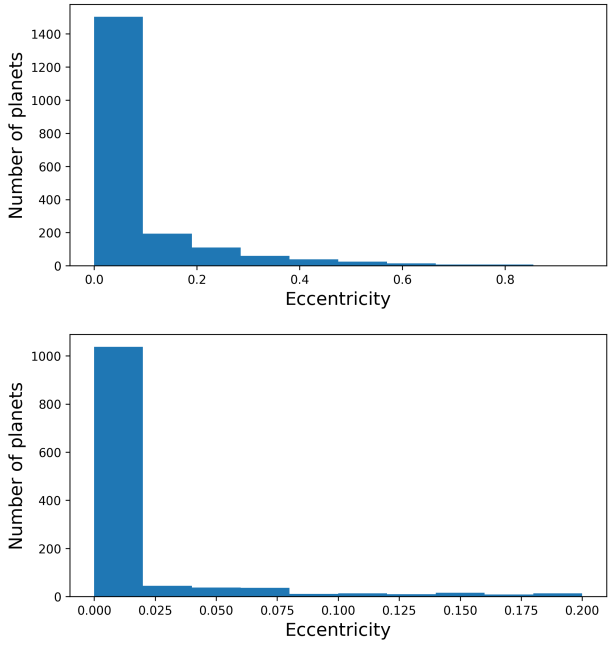

Figure 8: Graphics made with the catalogue used in our code. Both represents the number of planets, as a function of their eccentricity, for all systems (on the upper graph) and for the filtered data (on the lower graph).

5 Results

We present in this section the different results that we obtained.

5.1 General overview

Before discussing the results, it might be useful to recall that PPEs imply the alignment of three objects, in the direction of the line of sight. These events are thus extremely rare. The majority of the systems presented probabilities between 0.01% and 0.1%.

5.2 Obliquity known for every planets

Figure 9 presents the probability for the star HD-3167 to detect a PPE between planets b and c. The y-axis is repredented on a logarithmic scale for clarity.

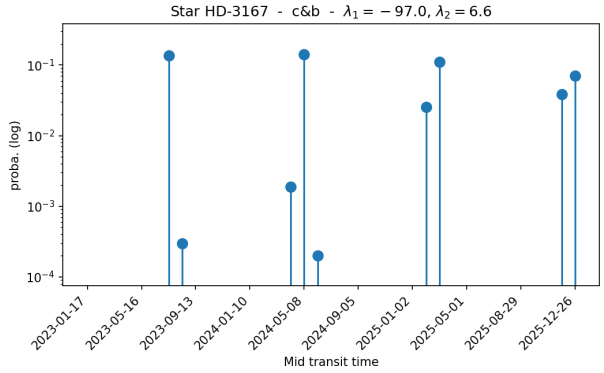

Figure 9: Probability to detect a PPE for HD-3167, between planets c and b, as a function of time. The probabilities are shown on a logarithmic scale.

One can observe some maximal values around 10% probabilities of PPE detection, which is rather high for such events. One can see that the probabilities are grouped in time, which could be explained by the fact that, in some cases, the revolution periods of exoplanets can be related with two integers ($nP_2 = mP_1$), meaning that, every nP_2 intervals of time, both planets will be in front of the stellar disc simultaneously after that planet 1 has made m revolutions around the star. Fig. 10 shows the results obtained for the star HD-63433, between planets b and c.

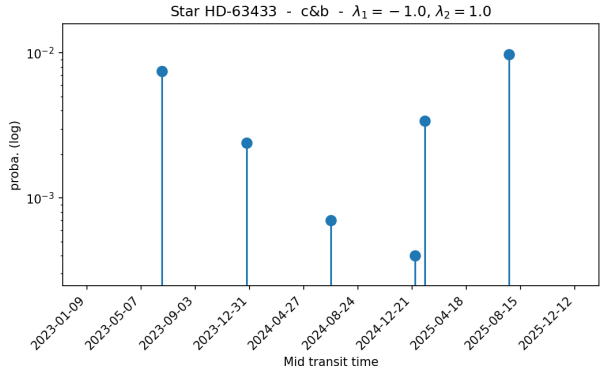

Figure 10: Same as Fig. 9 for the star HD-63433, between planets b and c.

As one can observe, the probabilities seem to decrease before increasing suddenly. This effect could be explained with the fact that, unlike what was explained for Fig. 9, the revolution periods cannot be related with integers, meaning that one has to wait $(n+1)P_2/P_1$ to get an integer again.

Results for TRAPPIST-1

We now present the results obtained for the star TRAPPIST-1. This system is made of 7 exoplanets, which make it very interesting for the detection of PPEs. Indeed, Fig. 11, taken from [5], illustrates the architecture of the system, as it is seen from Earth, rescaled at a factor 100:1 in the y-axis. As one can observe, this system is very compact in the inclinations. There seems to be two distinct groups between planets b, c, d, e, and planets f, g, h. This has been observed in our results, as the probabilities of PPE detection were much higher between planets belonging in the same group.

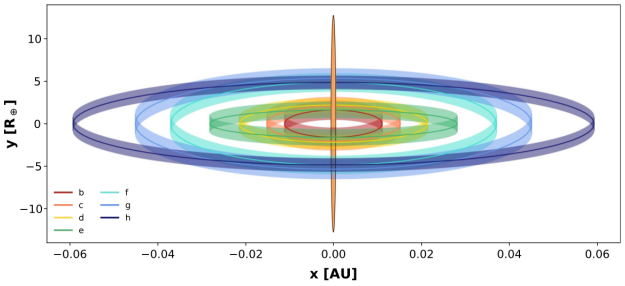

Figure 11: An illustration of the system made from TRAPPIST-1, and its seven orbiting planets. The configuration of the orbits is drawn as it would be seen from Earth. The scheme is scaled with a factor 100:1 on the y-axis for readability. Each solid line corresponds to a planetary orbit, and the transparent paths correspond to the planetary diameters. As one can observe, planets seems to be clustered in two groups between planets b, c, d, e, and planets f, g, h. This figure is taken from [5].

In Fig. 12, 13 and 14, we present three examples of results that we obtained for planets b, c, and d. The probabilities reaches some maximal values around 10%. One can really see that the probability curves evolve in a periodic way, which is surely due to the ratios between the periods of exoplanets.

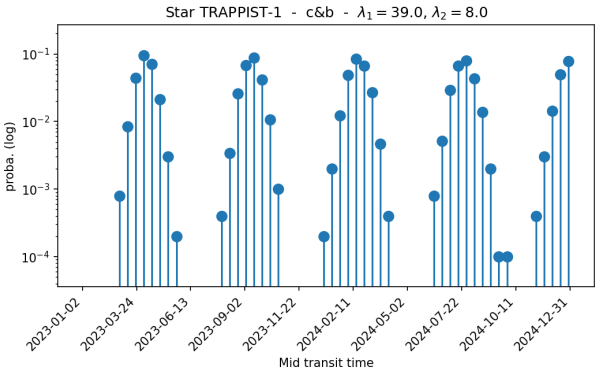

Figure 12: Same as Fig. 9 for the star TRAPPIST-1, between planets c and b.

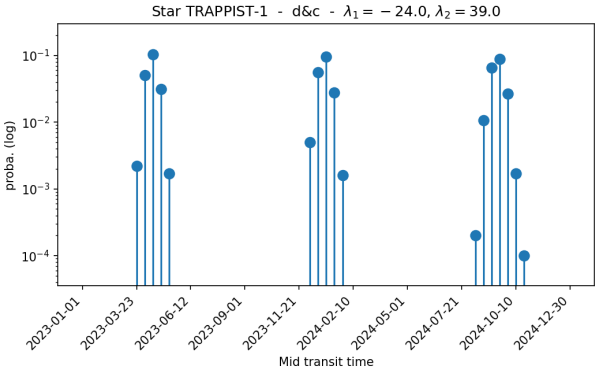

Figure 13: Same as Fig. 9 for the star TRAPPIST-1, between planets c and d.

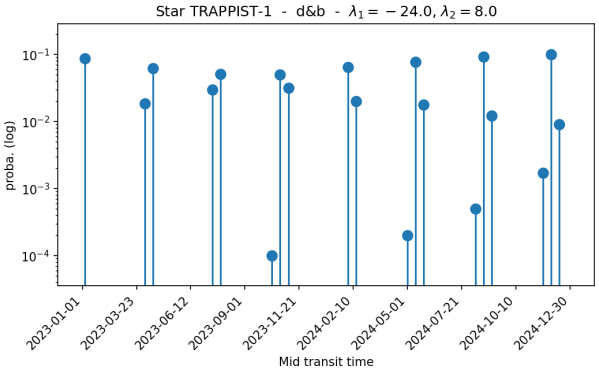

Figure 14: Same as Fig. 9 for the star TRAPPIST-1, between planets b and d.

On the last graph, one can see a sort of pattern evolving, that could be interpreted in the same way as explained for Fig. 10 with the relation between the revolution periods of the exoplanets. The peak of probability is thus shifted due to the difference in phase. Fig. 15 shows the results obtained for planets f and g :

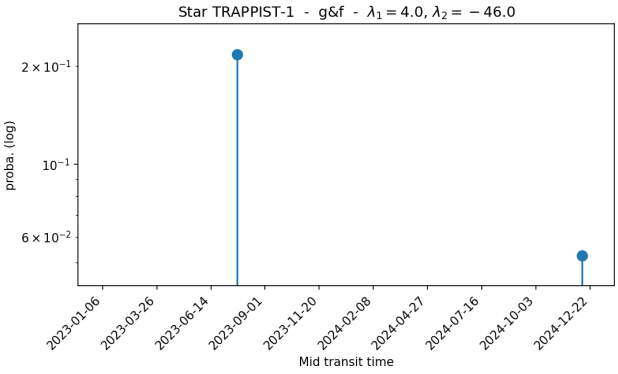

Figure 15: Same as Fig. 9 for the star TRAPPIST-1, between planets f and g.

As one can observe, the graph presents a probability detection of approximatively 20% on July 27th 2023, which is extremely high for such events. This graph shows the highest result that we were able to obtain with the data. Such a high result could be used in order to motivate the planning of an observation with space-based telescopes such as CHEOPS [12] or JWST [13]. It illustrates the biggest motivation of this work : we are able to predict where and when to observe the sky in order to have the highest chances to detect PPEs in the transit light curves.

5.3 Obliquity known for at least one planet

We now present an example of result for a pair of planets for which we did not know one of the obliquities. As the number of systems on which to compute the probabilities was very large, we decided to compute the probabilities between 2023 and 2025. Fig. 16 illustrates the probabilities to detect a PPE for the star Kepler-9, between planets b and c. As the obliquity of planet b is known ($\lambda_2 = -13.00$), we ran the code five times with different values for λ_1 according to eq. (3) : $\lambda_1 = [-103.0°\ ,\ -58.0°\ ,\ -13.0\ ,\ 32.0°\ ,\ 77.0°]$. These results show an evolution in the probability to observe a PPE. These graphs have to be considered with care, as they represent the probabilities for hypotetic values of the obliquity λ_1. An example of application of this method would be to run the code for a large number of values for λ_1. If these graphics present a peak of probability for a certain value of λ_1, and a PPE has effectively been observed, one could use these results in order to find a range of possible candidates for the real value of the obliquity λ_1.

6 Conclusion

In this work, we presented an approach based on Monte Carlo sampling in order to compute the probability to detect a planet-planet eclipse, given the orbital parameters of the planets. Even if such events are extremely rare, we were able to find encouraging results for systems like HD-3167 and TRAPPIST-1, whose probabilities reach peaks around 10% or 20%. This software offers the opportunity to evaluate where to observe in order to have the highest chances to observe PPEs, and could be used in order to plan observations missions with space telescopes. This code will also present more precise probabilities as the values in the catalogues will be updated, and show more results when new exoplanets will be detected.

References

[1] Darin Ragozzine and Matthew J. Holman. The Value of Systems with Multiple Transiting Planets, June 2010. Number: arXiv:1006.3727 arXiv:1006.3727 [astro-ph].

[2] E. Agol, J. Steffen, R. Sari, and W. Clarkson. On detecting terrestrial planets with timing of giant planet transits. *Monthly Notices of the Royal Astronomical Society*, 359(2):567–579, May 2005.

[3] Matthew J. Holman and Norman W. Murray. The Use of Transit Timing to Detect Extrasolar Planets with Masses as Small as Earth, December 2004. arXiv:astro-ph/0412028.

[4] Teruyuki Hirano, Norio Narita, Bun'ei Sato, Yasuhiro H. Takahashi, Kento Masuda, Yoichi Takeda, Wako Aoki, Motohide Tamura, and Yasushi Suto. Planet-Planet Eclipse and the Rossiter-McLaughlin Effect of a Multiple Transiting System: Joint Analysis of the Subaru Spectroscopy and the Kepler Photometry. *The Astrophysical Journal*, 759(2):L36, November 2012. arXiv:1209.4362 [astro-ph].

[5] Rodrigo Luger, Jacob Lustig-Yaeger, and Eric Agol. Planet–Planet Occultations in TRAPPIST-1 and Other Exoplanet Systems. *The Astrophysical Journal*, 851(2):94, December 2017.

[6] Joshua N. Winn. Transits and Occultations, September 2014. arXiv:1001.2010 [astro-ph].

[7] Heather A. Knutson, David Charbonneau, Robert W. Noyes, Timothy M. Brown, and Ronald L. Gilliland. Using Stellar Limb-Darkening to Refine the Properties of HD 209458b. *The Astrophysical Journal*, 655(1):564–575, January 2007.

[8] Nader Haghighipour. *Rossiter-McLaughlin Effect*, pages 2217–2220. Springer Berlin Heidelberg, Berlin, Heidelberg, 2015.

[9] The extrasolar planets encyclopaedia. `http://exoplanet.eu/`. Accessed: 2022-11-30.

[10] NASA. Nasa exoplanet archive. `https://exoplanetarchive.ipac.caltech.edu/`. Accessed: 2022-11-30.

[11] Michaël Gillon, Amaury H. M. J. Triaud, Brice-Olivier Demory, Emmanuël Jehin, Eric Agol, Katherine M. Deck, Susan M. Lederer, Julien de Wit, Artem Burdanov, James G. Ingalls, Emeline Bolmont, Jeremy Leconte, Sean N. Raymond, Franck Selsis, Martin Turbet, Khalid Barkaoui, Adam Burgasser, Matthew R. Burleigh, Sean J. Carey, Aleksander Chaushev, Chris M. Copperwheat, Laetitia Delrez, Catarina S. Fernandes, Daniel L. Holdsworth, Enrico J. Kotze, Valérie Van Grootel, Yaseen Almleaky, Zouhair Benkhaldoun, Pierre Magain, and Didier Queloz. Seven temperate terrestrial planets around the nearby ultracool dwarf star TRAPPIST-1. *Nature*, 542(7642):456–460, February 2017.

[12] Willy Benz, Christopher Broeg, Andrea Fortier, Nicola Rando, Thomas Beck, Mathias Beck, Didier Queloz, David Ehrenreich, Pierre Maxted, Kate Isaak, Nicolas Billot, Yann Alibert, Roi Alonso, Carlos António, Joel Asquier, Timothy Bandy, Tamas Bárczy, David Barrado, Susana Barros, Wolfgang Baumjohann, Anja Bekkelien, Maria Bergomi, Federico Biondi, Xavier Bonfils, Luca Borsato, Alexis Brandeker, Martin-Diego Busch, Juan Cabrera, Virginie Cessa, Sébastien Charnoz, Bruno Chazelas, Andrew Collier Cameron, Carlos Corral Van Damme, David Cortes, Melvyn Davies, Magali Deleuil, Adrien Deline, Laetitia Delrez, Olivier Demangeon, Brice-Olivier Demory, Anders Erikson, Jacopo Farinato, Luca Fossati, Malcolm Fridlund, David Futyan, Davide Gandolfi, Antonio Garcia Munoz, Michaël Gillon, Pascal Guterman, Antonio Gutierrez, Johann Hasiba, Kevin Heng, Eduardo Hernandez, Sergio Hoyer, Laszlo Kiss, Zsolt Kovacs, Thibault Kuntzer, Jacques Laskar, Alain Lecavelier des Etangs, Monika Lendl, Amador López, Ivan Lora, Christophe Lovis, Theresa Lüftinger, Demetrio Magrin, Luca Malvasio, Luca Marafatto, Harald Michaelis, Diana de Miguel, David Modrego, Matteo Munari, Valerio Nascimbeni, Göran Olofsson, Harald Ottacher, Roland Ottensamer, Isabella Pagano, Roberto Palacios, Enric Pallé, Gisbert Peter, Daniele Piazza, Giampaolo Piotto, Alberto Pizarro, Don Pollaco, Roberto Ragazzoni, Francesco Ratti, Heike Rauer, Ignasi Ribas, Martin Rieder, Reiner Rohlfs, Frederic Safa, Mario Salatti, Nuno Santos, Gaetano Scandariato, Damien Ségransan, Attila Simon, Alexis Smith, Michael Sordet, Sergio Sousa, Manfred Steller, Gyula Szabó, Janos Szoke, Nicolas Thomas, Matthias Tschentscher, Stéphane Udry, Valérie Van Grootel, Valentina Viotto, Ingo Walter, Nicholas Walton, François Wildi, and David Wolter. The CHEOPS mission. *Experimental Astronomy*, 51(1):109–151, February 2021. arXiv:2009.11633 [astro-ph].

[13] Jonathan P. Gardner, John C. Mather, Mark Clampin, Rene Doyon, Matthew A. Greenhouse, Heidi B. Hammel, John B. Hutchings, Peter Jakobsen, Simon J. Lilly, Knox S. Long, Jonathan I. Lunine, Mark J. McCaughrean, Matt Mountain, John Nella, George H. Rieke, Marcia J. Rieke, Hans-Walter Rix, Eric P. Smith, George Sonneborn, Massimo Stiavelli, H. S. Stockman, Rogier A. Windhorst, and Gillian S. Wright. The James Webb Space Telescope. *Space Science Reviews*, 123(4):485–606, April 2006. arXiv:astro-ph/0606175.

Figures without any indication of the source were self-made. This work has made use of data obtained from or tools provided by the portal `exoplanet.eu` of The Extrasolar Planets Encyclopaedia, and has also made use of the NASA Exoplanet Archive, which is operated by the California Institute of Technology, under contract with the National Aeronautics and Space Administration under the Exoplanet Exploration Program.

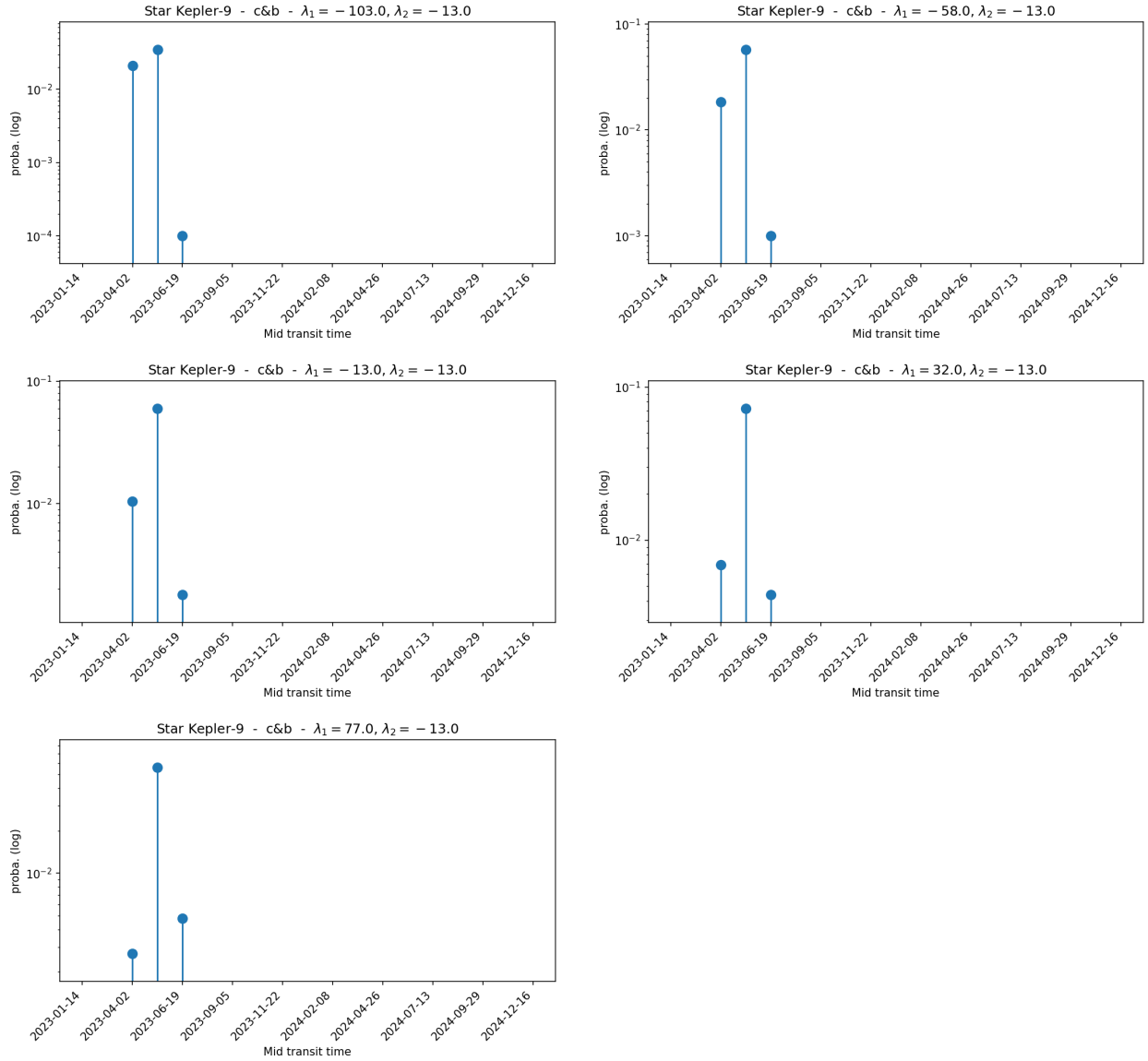

Figure 16: Logarithm of the probability of PPE detection as a function of time, for the star Kepler-9 between planets b and c. While the obliquity of b is $\lambda_2 = -13.0°$, we do not know the value λ_1 for planet c. We thus computed the probabilities for 5 different values of λ_1, according to formula (3) : $\lambda_2 = [-103.0°\ ,\ -58.0°\ ,\ -13.0\ ,\ 32.0°\ ,\ 77.0°]$.